Experimental investigation of phase change material (PCM) incorporated composite flat roof for energy-saving under Iraq hot climate conditions

Cite as: AIP Conference Proceedings **2404**, 080015 (2021); https://doi.org/10.1063/5.0069010
Published Online: 11 October 2021

Qudama Al-Yasiri and Márta Szabó

Experimental Investigation of Phase Change Material (PCM) Incorporated Composite Flat Roof for Energy-Saving under Iraq Hot Climate Conditions

Qudama Al-Yasiri [1, 2, 3, a)] and Márta Szabó [2, b)]

[1]*Mechanical Engineering Doctoral School, Hungarian University of Agricultural and Life Sciences, Páter K. u. 1, Gödöllő, H-2100, Hungary.*
[2]*Department of Building Services, Institute of Technology, Hungarian University of Agriculture and Life Sciences, Páter K. u. 1, Gödöllő, H-2100, Hungary.*
[3]*Department of Mechanical Engineering, Faculty of Engineering, University of Misan, Al Amarah City, Maysan, 62001, Iraq.*

[a)] Corresponding author: qudamaalyasiri@uomisan.edu.iq
[b)]Szabo.marta@uni-mate.hu

Abstract. The roof plays a predominant role in residential buildings' energy efficiency in hot countries as it receives a significant amount of solar radiation during the summer months. Incorporating phase change material is considered a sustainable solution to improve building energy performance. In this paper, the energy-saving earned from incorporating separate phase change material panel into a composite flat roof is investigated experimentally under hot climatic conditions of Al Amarah city, south of Iraq. Two identical small-scale rooms (with and without phase change material layer) have installed considering composite flat roof and insulated floor and walls. The roofs are composed of Isogam (as a roofing layer), concrete (as the main roof layer) and gypsum board (as a cladding layer). The maximum temperature reduction, average temperature fluctuation reduction, decrement factor and time lag have been calculated and discussed. Results indicated that PCM could efficiently reduce heat transfer through the roof and contribute to building energy-saving. The maximum interior surface temperature is reduced by up to 8.75 °C in the PCM roof. Moreover, an average maximum temperature reduction, average temperature fluctuation reduction, decrement factor and time lag of respectively 10.65%, 7.68 °C, 0.522 and ~100 min, is obtained from the modified roof compared to the reference roof.

INTRODUCTION

Globally, buildings are responsible for approximately 40% of end-use energy and a higher ratio of CO_2 emissions [1]. Besides, building envelope shares a higher percentage of this number by up to 36% due to construction and related renovation activities [2]. Therefore, governments and responsible authorities are aiming to enhance the efficiency of this key energy consumer.

Building roof is an essential element that influences the building envelope, especially in hot locations, because it exposes to higher solar radiation compared with other building envelope elements (i.e. walls and windows). Accordingly, building energy and thermal comfort are highly influence due to high cooling/heating loads. Various solutions are applied to improve the building roof's thermal performance, such as insulators, cool coating, greening, shading, double skin, thermal activation, etc. [3-6]. Incorporating phase change material (PCM) has recently been introduced as a promising technology, showing an advantage of storing and realising an immense amount of heat that regulates heat energy through the building roofs for both cooling and heating applications [7-10].

Several studies have investigated the potential of PCMs in building roofs, highlighting the contribution to building energy saving under different locations. Beemkumar et al. investigated the reduction of peak temperature and temperature fluctuations of a PCM roof compared to a roof without PCM (25 °C -28 °C melting temperature) under Chennai, India climatic conditions [11]. Outcomes showed that the peak temperature was reduced by 1–2 °C

2nd International Conference on Engineering & Science
AIP Conf. Proc. 2404, 080015-1–080015-9; https://doi.org/10.1063/5.0069010
Published by AIP Publishing. 978-0-7354-4136-1/$30.00

in the PCM roof, and the temperature fluctuations had reduced to be suitable for thermal comfort requirements. Beemkumar et al. analysed PCM's contribution (28 °C -30 °C melting temperature) incorporated roof in terms of average peak temperature reduction at the same climate conditions [12]. Two identical roofs - one with and without PCM - were built and compared concerning a numerical model run for five consecutive days assuming average climatic conditions. Results reported that the average peak temperatures in the PCM roof were reduced by 2–4°C. Moreover, the study concluded that increasing PCM thickness in the roof resulted in more energy-saving and thermal comfort at a constant temperature. Abuelnuor et al. studied two rooms of identical inner dimensions with and without PCM have 30 °C melting temperature under hot weather conditions of Khartoum, Sudan [13]. Experimental results showed that the interior temperature of the room built with PCM was reduced by 3-4 °C compared with the room without PCM. Yu et al. numerically studied the decrease of roof inner surface temperature and decrement factor of roof-based PCM layer under five Chinese weather conditions [14]. Building roof based shape-stabilised PCM at optimal melting temperature compared with a conventional roof. Results indicated that the optimal PCM melting temperature linearly increases with average outdoor solar air temperature. Therefore, the optimum PCM melting temperatures were 31~33°C, 34~36°C,36~38°C, 34~36°C, and 29~31°C respectively for the severe cold region, cold region, hot summer and cold winter region, hot summer and warm winter region, and mild region. In PCM roof compared with the conventional one, the decrement factors decreased by 85.90%, 87.12%, 85.78%, 87.83%, and 88.79%. Moreover, the corresponding peak roof interior surface temperatures were decreased by 3.7 °C, 4 °C, 3.9 °C, 3.8 °C, and 3.7 °C, respectively. Zhang et al. studied the effect of different roof types (including PCM roof) on energy saving under a controlled environment [15]. Experimental results showed that incorporating PCM into the roof can minimise the interior temperature by up to 6.6 °C. Furthermore, the study indicated the importance of optimal position and thickness of the PCM layer on the performance enhancement.

This work experimentally investigates the thermal performance of a popular Iraqi composite roof when adding a PCM layer. The roof comprises Isogam, concrete and gypsum board layer (from outside to inside), as they have a poor thermal performance to investigate the contribution of PCM. A comprehensive comparison was conducted between the popular (original) and the modified roofs to evaluate several energetic indicators such as the maximum temperature reduction, average temperature reduction, decrement factor and time lag.

MATERIALS AND METHODS

Experimental Rooms

Two identical test rooms were installed and tested under the weather conditions of Al Amarah city (Latitude: 31.84° & Longitude: 47.14°), Iraq. Both rooms were fabricated from a conventional flat composite roof combination known for its poor thermal performance. The first room (termed as R-A) was characterised as a reference room, whereas the other was the modified one with a PCM layer placed between the Isogam and concrete layer (termed as R-B) in Fig. 1. Both roofs were installed on the top of locally-made cork boxes with high thermal insulation to serve as the rooms' walls and floor. Boxes were covered with fibreglass blanket to improve sidewalls and floors' insulation, which guarantees that the heat passes only through the composite roofs. Moreover, all roof layers in both test rooms were appropriately placed one by one and sealed separately using good insulation foam to guarantee no air leakage between the inside and outside environments.

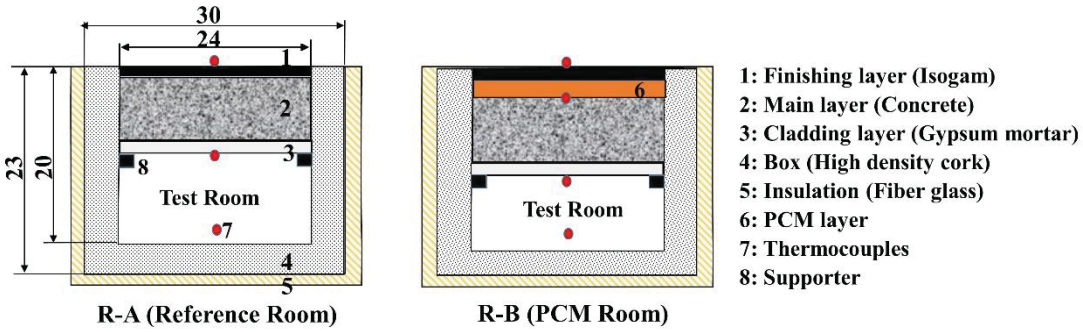

FIGURE 1. Schematic for the experimental rooms.

Composite Roof Layers

The conventional composite flat roof comprised of Isogam (0.4 mm thickness) as a finishing layer, concrete (50 mm thickness) as the main roof layer, and gypsum board (8 mm thickness) as a cladding layer. This roof combination is popular in the residential buildings in modern construction pattern and the chief responsible for buildings high cooling loads during the summer season [16].

Isogam is a popular layer used in the last 15 years as an alternative roofing layer due to its relatively low cost and good waterproof ability. This layer made from bitumen-rubber mastic covered with thin plastic from both sides (Fig. 2-a). One of these plastic layers is coated with reflective colours to reflect as much as possible of fallen solar radiation and minimise the heat transferred towards the indoor. The coated layer of Isogam is influencing by the changeable weather conditions, which decrease its time of service. Therefore, a considerable amount of heat is transmitting through the roofs after a few years of Isogam installation. In this work, the Isogam reflective layer was removed to examine the thermal performance of PCM under a high-temperature range and the contribution of the PCM layer to the energy-saving.

The concrete layer was fabricated from local conventional raw materials, namely Portland cement, sand and gravel (Fig. 2-b). It was made according to the mixing ratio (1:2:4), which is popular to produce a roof layer with a compressive strength of 25-30.

A pre-fabricated gypsum board was used as a cladding layer, which is popular in Iraqi buildings. This type of boards are available in the local market and used mainly for decoration purposes (Fig. 2-c).

FIGURE 2. Composite roof layers (a) Isogam (b) Concrete (c) Gypsum (d) PCM.

PCM Layer

An additional PCM layer was inserted in the composite roof of R-B between Isogam and concrete layers. The panel was made with 10 mm thickness from galvanised steel sheet (0.4 mm thickness), which is available in the market at low cost and compatible with a wide range of PCMs in terms of corrosiveness [18] (Fig. 2-d). According to our previous work, this PCM layer thickness is enough to ensure the melting and solidification phases during the experiment days [19]. Moreover, this type of macroencapsulation materials is preferred to provide good thermal performance for PCM during melting and solidification [20]. In this work, paraffin wax (500 g) served as a PCM. The PCM was melted and poured inside the panel to create a shape-stabled and efficient PCM layer with higher thermal conductivity.

The used PCM is popular in the country and produced in the Iraqi refineries during the dewaxing of crude oil [21]. Moreover, paraffin wax generally has good thermophysical properties (except the low thermal conductivity) to serve as a PCM in thermal energy storage applications. The general properties of used PCM are listed in Table 1.

TABLE 1. Properties of PCM [22].

Appearance	Thermal conductivity (W/m.K)	Latent heat of fusion (kJ/kg)	Density (kg/m^3)	Specific heat (kJ/kg.K)
White	0.21	190	930 (solid) 830 (liquid)	2.1

Instrumentation

The experimental work was performed over three consecutive days (7-9/9/2020), from 6:00. Seven thermocouples (of T-type) were used to measure the temperature with 10 min time step. The thermocouples were connected to a data logger work-based multi-channel Arduino (Mega 2560 type) in which the collected data were stored inside storage memory. A mobile solar power meter was used to collect SR manually every 30 min. The specifications of instruments used in the experimental work are listed in Table 2.

TABLE 2. Specifications of instruments.

Instrument	Model	Range	Resolution	Accuracy
Thermocouples T-type (0.2 mm)	TEMPSENS	-270 °C – 370 °C	----------	+/- 0.5 °C
Solar power meter	SM206	0.1~399.9 W/m^2	0.1 W/m^2	±10 W/m^2

Thermocouples are fixed in four positions: on the outer finishing layer, below the PCM layer, below the cladding layer and inside the test room, as indicated in Fig. 1. Fig. 3 shows the experimental models and the measurement devices.

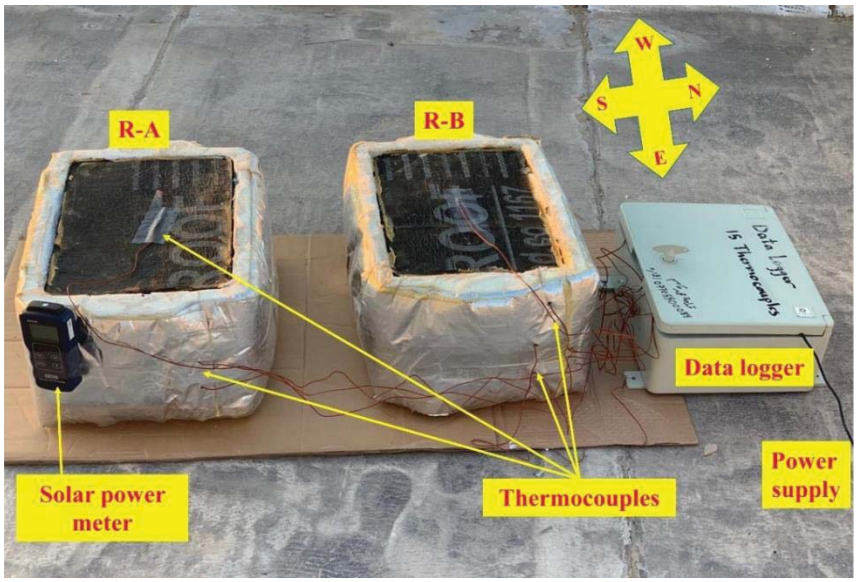

FIGURE 3. Experimental rooms.

Evaluation of Energy-Saving

Four indicators have been introduced to evaluate the energy-saving obtained from the PCM in R-B compared with the reference roof. These indicators are considering the reduction of the room temperature (T_r) and interior surface temperature (T_i) compared to the average exterior surface temperature of the roof (To) during days of an experiment to identify each indicator value. The indicators are the maximum temperature reduction, average temperature fluctuation reduction, decrement factor and time lag.

The maximum temperature reduction (MTR) indicator shows the maximum reduction of R-B room temperature than R-A during peak hour. Therefore, this indicator indicates the contribution of the PCM layer to an energy-saving of the composite roof. MTR can be calculated considering the maximum room temperature of R-A and R-B, according to Eq. (1), as follows:

$$MTR = \frac{T_{r,max.,R-A} - T_{r,max.,R-B}}{T_{r,max.,R-A}} \times 100\% \quad (1)$$

where $T_{r,max,R-A}$ and $T_{r,max,R-B}$ are the maximum room temperature of R-A and R-B (°C).

Average temperature fluctuation reduction (ATFR) is the average decrease in roof fluctuations during the experiment period. ATFR calculated by uniting the average decrease in room temperature (indoor temperature) during day hours (considered from 6:00 - 18:00 as X) with the average increase in room temperature during the night hours (considered from 18:00 to the end of the day as Y), according to Eq. (2)-Eq. (4), as follows [23]:

$$ATFR = X + Y \quad (2)$$

$$X = T_{r,av.,R-A} - T_{r,av.,R-B} \quad (3)$$

$$Y = T_{r,av.,R-B} - T_{r,av.,R-A} \quad (4)$$

where $T_{r,av.,R-A}$ and $T_{r,av.,R-B}$ are the average temperature of the R-A and R-B (°C).

Decrement factor (DF) decreases peak temperature in composite roof layers considering the inside and outside roof surface temperatures. This indicator shows the thermal resistance of roof layers against the transferred heat. Therefore, it can be calculated by Eq. (5), as follows [24]:

$$DF = \frac{T_{i,max} - T_{i,min}}{T_{o,max} - T_{o,min}} \quad (5)$$

where $T_{i,max}$, $T_{i,min}$, $T_{o,max}$ and $T_{o,min}$ are the maximum and minimum temperatures of the interior and exterior roof surfaces (°C). Accordingly, the lower DF indicates lower temperature fluctuations within the roof layers.

Time lag (TL) is the time difference between the maximum exterior and interior roof surface temperatures. This indicator is important to show how much the peak load is shifted during the day. TL can be calculated by subtracting the time at a maximum interior surface temperature from the time at maximum exterior surface temperature, according to Eq. (6) [25], as follows:

$$TL = \tau_{T_{i,max}} - \tau_{T_{o,max}} \quad (6)$$

where $\tau_{Ti,max}$ and $\tau_{To,max}$ are the time at the maximum interior and exterior roof surface temperatures (min), respectively.

All the above indicators are necessary to evaluate the energy-saving earned from incorporating the PCM layer into the composite flat roof.

RESULTS AND DISCUSSION

The measurements lasted for three consecutive hot days of summer 2020 in one of the hottest months in Iraq (i.e., September). Fig. 4 shows the average daily weather conditions in September, reflecting the behaviour of ambient temperature ($T_{amb.}$) and solar radiation (SR) in the experiment days.

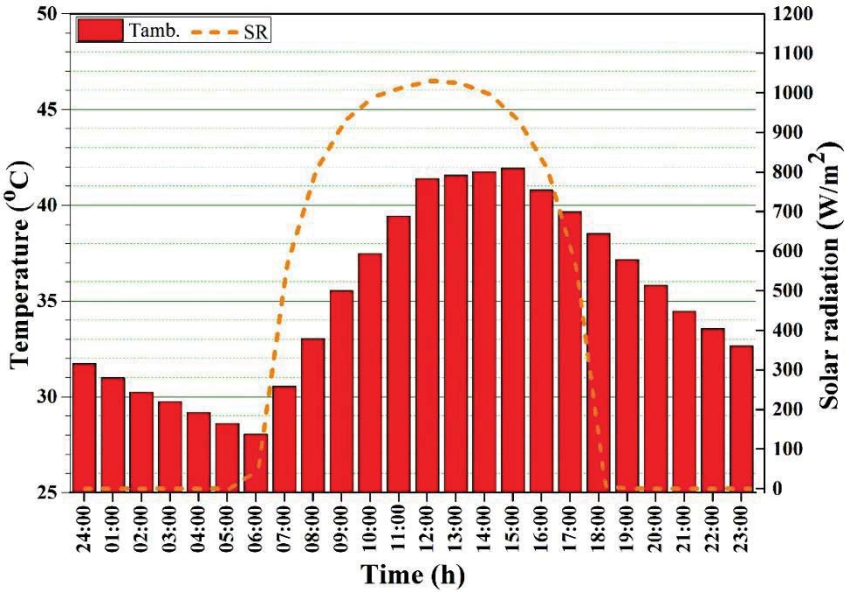

FIGURE 4. Average daily ambient temperature and solar radiation during September [26].

Fig. 5 shows the temperature profile of the experimental rooms (R-A and R-B) in terms of time and solar radiation during the experiment. It is noted that T_i and T_r increased as T_o increase, which reached a maximum of 71.6 °C, 76.8 °C and 73.9 °C respectively in the 1st, 2nd and 3rd of the experimental days at a highest solar radiation of 1098, 1215 and 1133 W/m2 in midday. Besides, T_i and T_r values in R-B are remarkably lower than those in R-A, indicating the PCM layer's role in shaving the heat transferred in the direction of the test room and worked as a heat barrier.

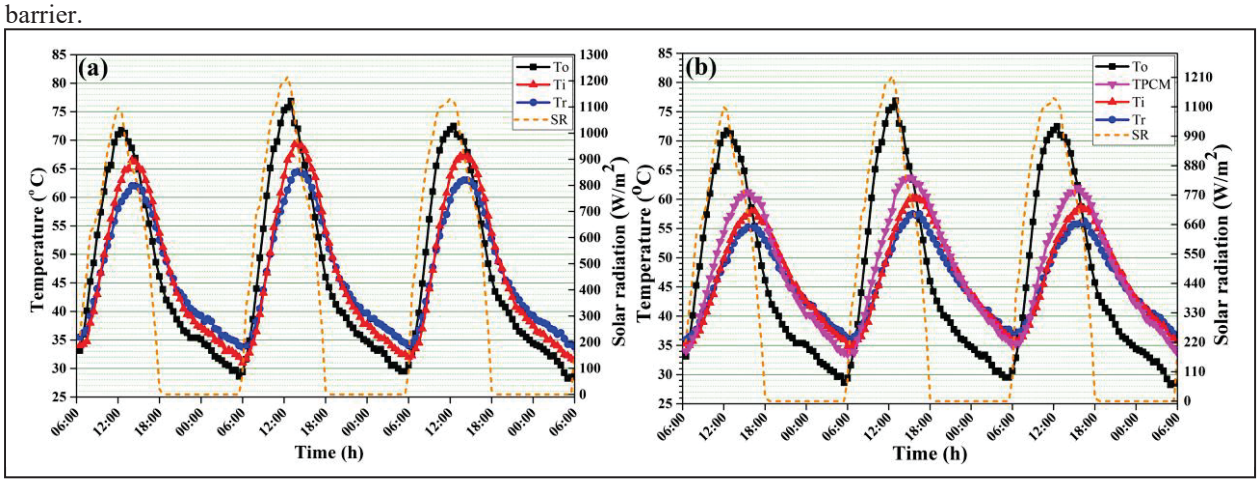

FIGURE 5. Temperature profile of tested roofs (a) R-A, (b) R-B.

T_i and T_r were increasing in the first half of each cycle as T_o increase and reached a maximum in the mid-afternoon for R-A and late afternoon for R-B considering the time delay caused by the PCM layer. In the second half of the day cycle, T_o was decreasing sharply influenced by the fallen solar radiation although the high absorptivity of Isogam layer and high ambient temperature. Accordingly, T_i and T_r were decreasing slowly (compared to the rapid decrease of To) due to composite roof layers resistance and non-conditioned case. During the night period up to the beginning of the next day, T_o values were fallen below 30 °C, which were suitable for discharging heat from both composite roofs, particularly for R-B. Therefore, the PCM was prepared for the next day cycle.

As indicated in subsection 2.3, several indicators were defined to evaluate the PCM layer incorporation's benefits. Considering the test room temperature in both R-A and R-B, T_o was reduced remarkably through the composite roofs, especially in R-B, as shown in Fig. 6. T_r was reduced significantly in R-B compared with R-A in all

cycles. Accordingly, the MTR for R-B compared with R-A was reached up to 10.44%, 10.85% and 10.67% in the first, second and third cycles, respectively, as shown in Fig. 6.

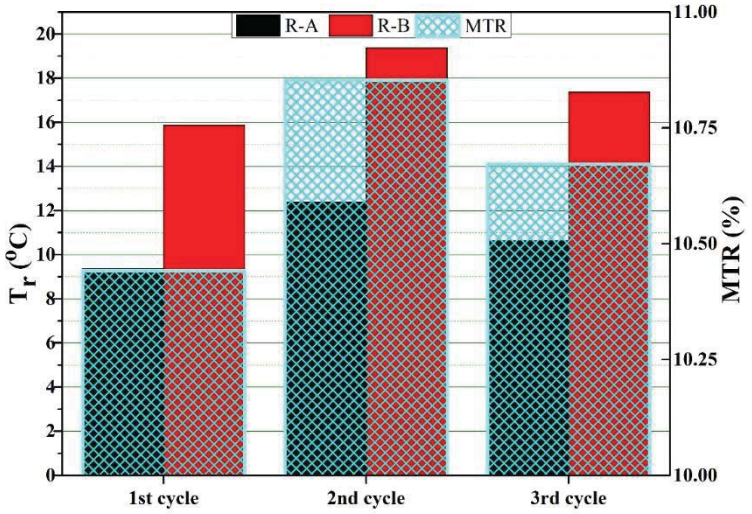

FIGURE 6. MTR of R-B considering the maximum reduction of T_r.

The figure above showed that MTR in the second cycle is the highest, followed by the third cycle, indicating that PCM worked better at high To. This is attributed to the high melting temperature of used PCM, which is more efficient under high temperatures.

ATFR indicates the average temperature reduction in the composite roofs; in this sense, all T_r should be considered, as shown in Fig. 7.

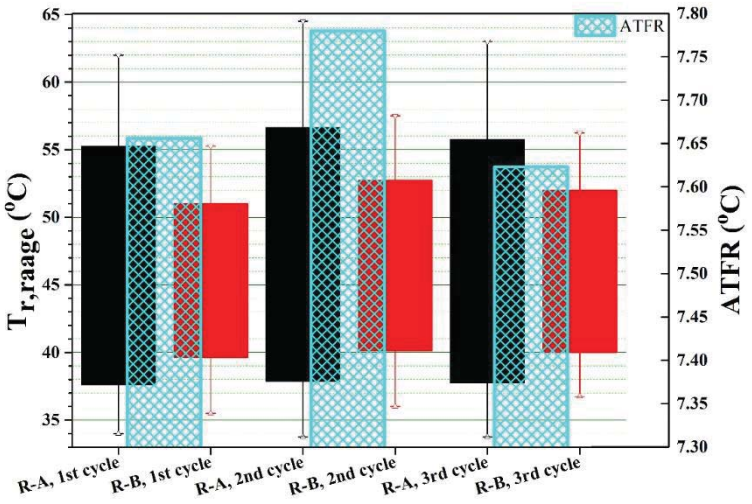

FIGURE 7. ATFR of R-B in terms of average T_r.

The results of ATFR designated a high thermal performance of PCM wherein the values in the range 7.62 °C < ATFR < 7.78 °C, and they are better than the results reported in the literature studies. For example, a study conducted by Alam et al. reported that ATFR ranged between 3-4 °C under the climate conditions of Australia [27].

Fig. 8 shows the DF of experimental roofs, indicating a relatively high decrease in R-B interior surface temperature compared with R-A.

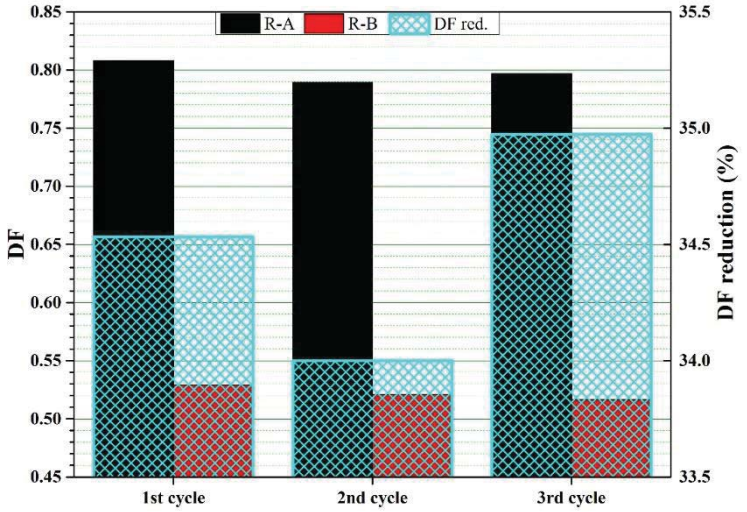

FIGURE 8. DF and DF reduction of R-A and R-B.

DF was calculated as 0.808, 0.789 and 0.797 for R-A and 0.529, 0.521 and 0.516 for R-B in the first, second and third cycles. This means that the cyclic interior surface temperature of R-B was reduced by 34.53%, 34% and 34.97% in the first, second and third cycles. The maximum DF reduction was reported for the third cycle due to lower temperature variation (T_i and T_r (Fig. 7)) compared with the other cycles.

All cycles showed a remarkable shifting of peak temperature for at least 90 min in R-B compared with R-A for TL indicator. The calculated TL in both rooms is shown in Fig. 9.

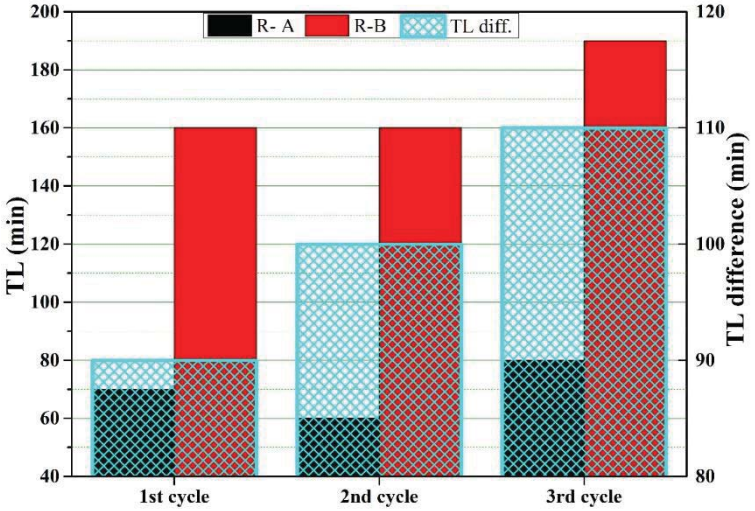

FIGURE 9. TL and TL difference between R-A and R-B.

TL was increased for R-B by 90, 100 and 110 min compared with R-A. This time increment is attributed to PCM's potential that stores the transferred heat through the roof, which is the primary purpose of PCM of shaving and shifting the peak load in building applications.

The latter two indicators (i.e., DF and TL) are essential to analyse PCM's thermal performance on the building envelope as they determine its thermal resistance against the high outside temperatures [28].

CONCLUSION

In this work, the energy-saving earned from incorporating a macroencapsulated PCM into a composite flat roof is studied experimentally under Iraq's hot climate conditions. Experimental results for two non-conditioned rooms are

presented in terms of four indicators to show PCM's energy contribution and potential to the composite roof thermal behaviour. The study demonstrated that PCM could be used as a passive solution under Iraqi weather conditions considering the high exterior temperature at night. In this regard, the peak temperature is shaved and shifted remarkably using PCM inside the composite roof even under high exterior surface temperatures. Moreover, an average MTR, ATFR, DF and TL of respectively 10.65%, 7.68 °C, 0.522 and ~100 min, is obtained for PCM composite roof compared to the one without PCM.

ACKNOWLEDGEMENTS

This work was supported by the Stipendium Hungaricum Programme and the Doctoral School of Mechanical Engineering, Hungarian University of Agriculture and Life Sciences, Gödöllő campus, Hungary.

REFERENCES

1. International Energy Agency, "CO_2 Emissions from Fuel Combustion", (2020).
2. International Energy Agency and UN Environment Programme, "2019 global status report for buildings and construction: Towards a zero-emission, efficient and resilient buildings and construction sector", (2019).
3. H. Radhi, S. Sharples, H. Taleb, and M. Fahmy, *Energy Build.*, 135, 324–337 (2017).
4. M. Mahmoodzadeh, P. Mukhopadhyaya, and C. Valeo, *Water*, 12, 6 (2020).
5. K.T. Zingre, E.H. Yang, and M.P. Wan, *Energy*, 133, 900–912 (2017).
6. B. Behrendt, "Possibilities and Limitations of Thermally Activated Building Systems Simply TABS and a Climate Classification for TABS", Ph.D. thesis, Technical University of Denmark, 2016.
7. Q. Al-Yasiri and M. Szabó, *J. Build. Eng.*, 36, 102122 (2021).
8. C. Piselli, V.L. Castaldo, and A.L. Pisello, *Sol. Energy*, 192, 106–119 (2019).
9. E. Tunçbilek, M. Arıcı, S. Bouadila, and S. Wonorahardjo, *J. Therm. Anal. Calorim.*, 141, 613–624 (2020).
10. Q. Al-Yasiri and M. Szabó, *Eur. J. Energy Res.*, 1, 7–14 (2021).
11. N. Beemkumar, D. Yuvarajan, M. Arulprakasajothi, K. Elangovan, and T. Arunkumar, *J. Therm. Anal. Calorim.*, 30, 101536 (2020).
12. N. Beemkumar, D. Yuvarajan, M. Arulprakasajothi, S. Ganesan, K. Elangovan, and G. Senthilkumar, *J. Sol. Energy Eng. Trans. ASME*, 142, (2020).
13. A.A.A. Abuelnuor, I.H.I. Alhag, A.A.M. Omara, M.K. Awad, and M.H. Mohammed, "Buildings cooling: An experimental study of Phase Change Materials storage for low energy buildings", in: 2017 Int. Conf. *Commun. Control. Comput. Electron. Eng.*, (2017), pp. 1–5.
14. J. Yu, Q. Yang, H. Ye, J. Huang, Y. Liu, and J. Tao, *Energy Procedia*, 158, 3045–3051 (2019).
15. Y. Zhang, J. Huang, X. Fang, Z. Ling, and Z. Zhang, *Int. J. Energy Res.*, 44, 1594–1606 (2020).
16. Q. Al-Yasiri, M.A. Al- Furaiji, and A.K. Alshara, *J. Eng. Technol. Sci.*, 51, 632–648 (2019).
17. M. Moslah Salman and M. Zohair Yousif, *J. Eng. Sustain. Dev.*, 22, 116–130 (2018).
18. G.H. Feng, D. Liang, K.L. Huang, and Y. Wang, *Sustain. Cities Soc.*, 50, 101662 (2019).
19. Q. Al-Yasiri and M. Szabó, *Case Stud. Constr. Mater.*, 14, e00522 (2021).
20. Q. Al-Yasiri and M. Szabó, Int. J. Green Energy, 18 (9), 966-986 (2021).
21. H.J. Akeiber, M.A. Wahid, H.M. Hussen, and A.T. Mohammad, *Energy*, 104, 99–106 (2016).
22. M.T. Chaichan, A.H. Al-Hamdani, and A.M. Kasem, *Int. J. Sci. Eng. Res.*, 7, 736–741 (2016).
23. S. Kenzhekhanov, S.A. Memon, and I. Adilkhanova, *Energy*, 192, 116607 (2020).
24. C. Sun, S. Shu, G. Ding, X. Zhang, and X. Hu, *Energy Build.*, 61, 1–7 (2013).
25. M. Arıcı, F. Bilgin, S. Nižetić, and H. Karabay, *Appl. Therm. Eng.*, 165, 114560 (2020).
26. PVGIS: European Comunities, https://ec.europa.eu/jrc/en/pvgis .
27. M. Alam, H. Jamil, J. Sanjayan, and J. Wilson, *Energy Build.*, 78, 192–201 (2014).
28. P.M. Toure, Y. Dieye, P.M. Gueye, V. Sambou, S. Bodian, and S. Tiguampo, *Case Stud. Constr. Mater.*, 11, e00298 (2019).